Online monitoring of the kinetic isotope effect in chemical reactions with ^{1}H and ^{19}F low-field NMR spectroscopy

Kawarpal Singh and Bernhard Blümich

Supplementary Information

Table of Contents

1 Compact NMR spectrometer at 1 T

a)   b)
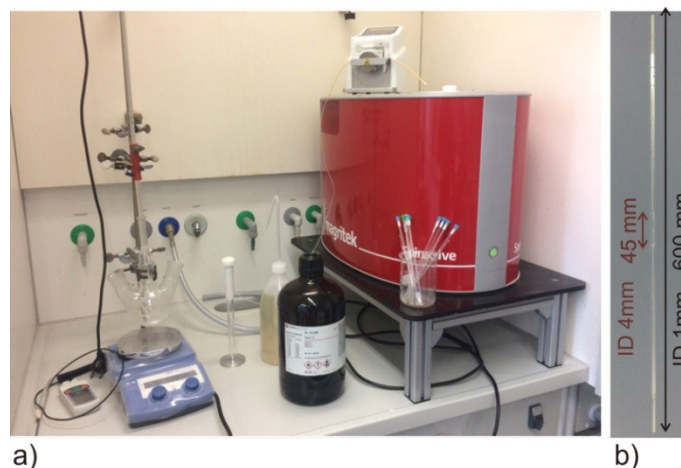
Figure S1: Experimental setup. a) Desktop 1T NMR spectrometer and reaction setup inside the fume hood. b) Flow cell used to pass the reaction mixture through the magnet using the PTFE tubing.

a)   b)
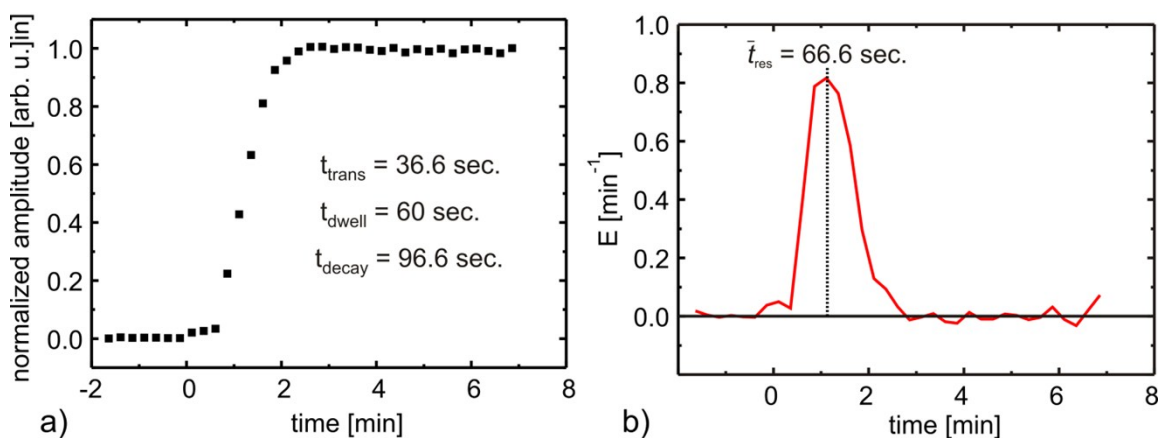
Figure S2: a) Signal response of acetone after adding acetone at $t = 0$ min to the reactor containing isopropanol. b) Residence time distribution function for compact NMR at 1 T.

2 Residence-time distribution and signal response

3   Longitudinal relaxation times for educts and products of acetic anhydride hydrolysis reaction
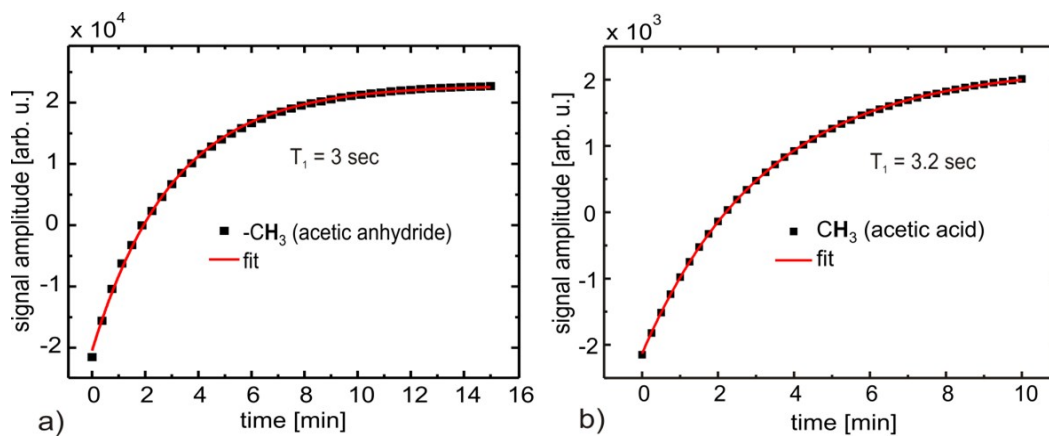
Figure S3: Longitudinal relaxation times of different protons. a) Methyl protons (acetic anhydride). b) Methyl protons (acetic acid).

4 Longitudinal relaxation times for educts and products of ethyltrifluoroacetate
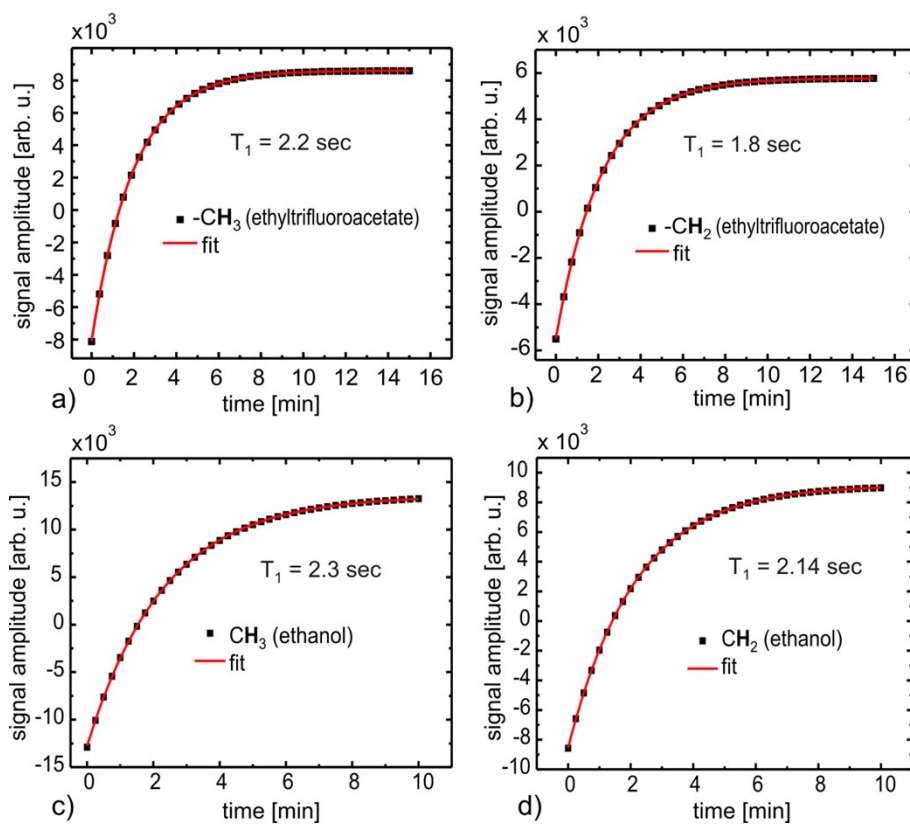
Figure S4: Longitudinal relaxation times of different protons. a) Methyl protons (ethyl trifluoroacetate). b) Methylene protons (ethyl trifluoroacetate). c) Methyl protons (ethanol). d) Methylene protons (ethanol).

5 Stack plot of 1D ^{1}H NMR spectra for acetic anhydride hydrolysis
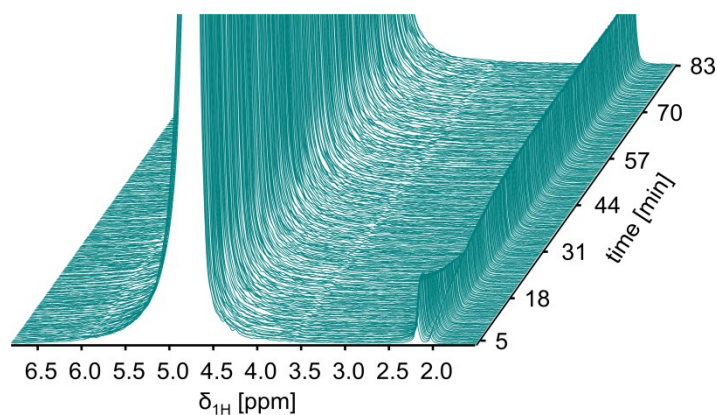
Figure S5: Stack plot of 1D ^{1}H NMR spectra acquired during the 90-minute hydrolysis of acetic anhydride (0.18 mol L^{-1}) in H_2O at 294 K with an agitation speed of 200 rpm and a flow rate of 1 ml/min.

6 Calibration curve of acetic anhydride
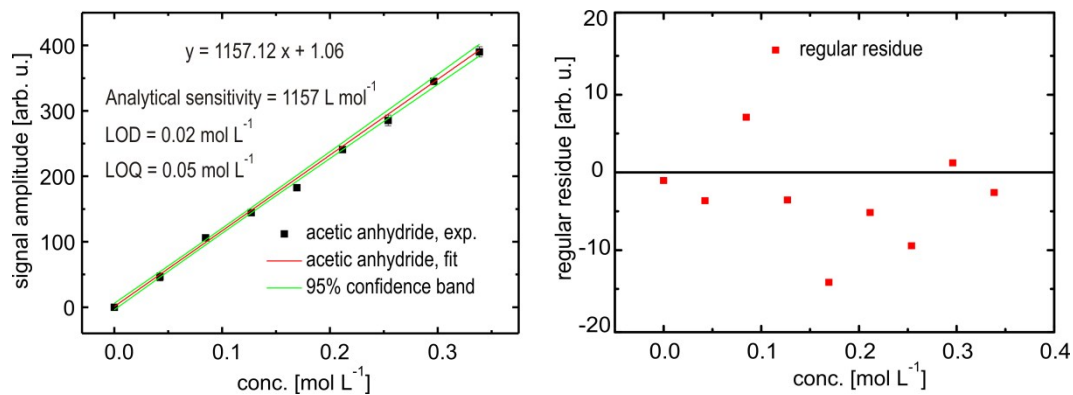
Figure.S6: a) Calibration curve corresponding to acetic anhydride. b) Distribution of the residuals.

7 Transition state structure of rate-determining step of hydrolysis reactions
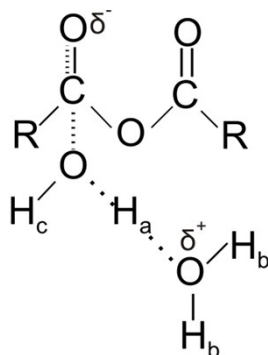
Figure S7: Transition state model for the hydrolysis reactions obtained by studying the proton inventory effects.[33]

8 Stack plot of 1D NMR ^{1}H and ^{19}F NMR for ethyltrifluoroacetate hydrolysis
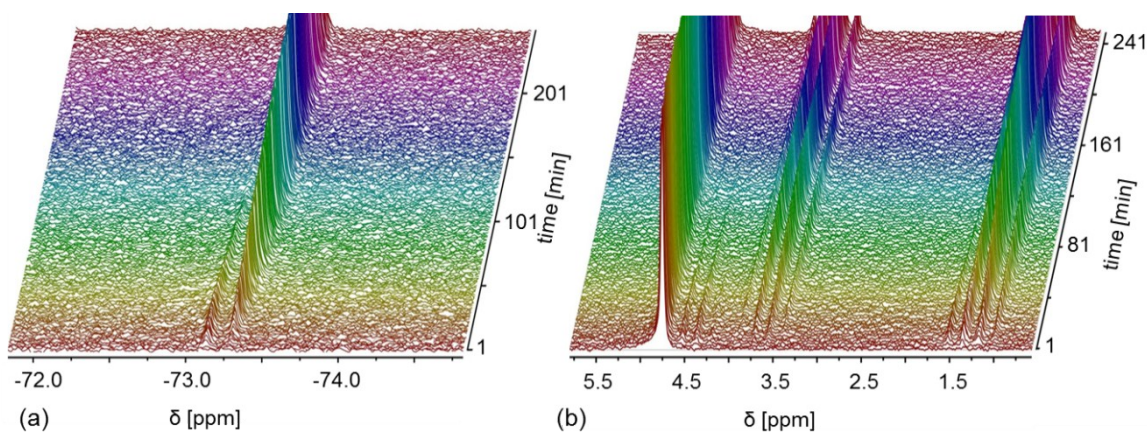
Figure S8: Stack plots of 1D NMR spectra acquired during 4 hours for the hydrolysis of ethyl trifluoroacetate (0.08 molL-1) in D_2O at 296 K with an agitation speed of 200 rpm and a flow rate of 1 ml/min. a) 1D ^{19}F spectra. b) 1D ^{1}H spectra.

9   Calibration curve of ethyltrifluoroacetate
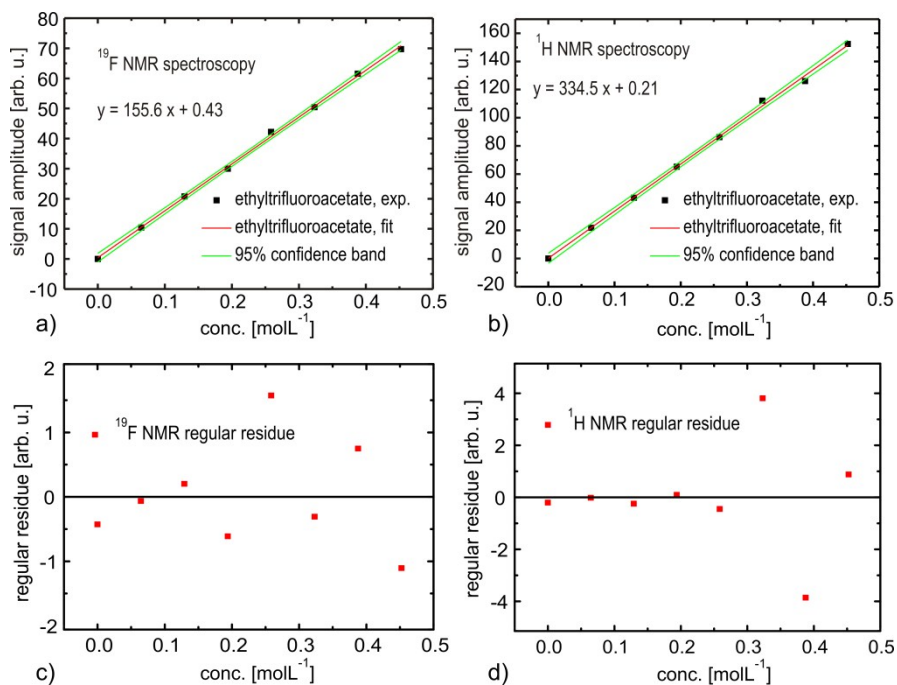
Figure S9: Calibration curves corresponding to ethyltrifluoroacetate. a) ^{19}F NMR spectroscopy. b) ^{1}H NMR spectroscopy. Distribution of residuals. c) ^{19}F NMR spectroscopy. d) ^{1}H NMR spectroscopy.

10 Temperature dependence of ethyl trifluoroacetate obtained using 1D ^{1}H and ^{19}F NMR spectroscopy
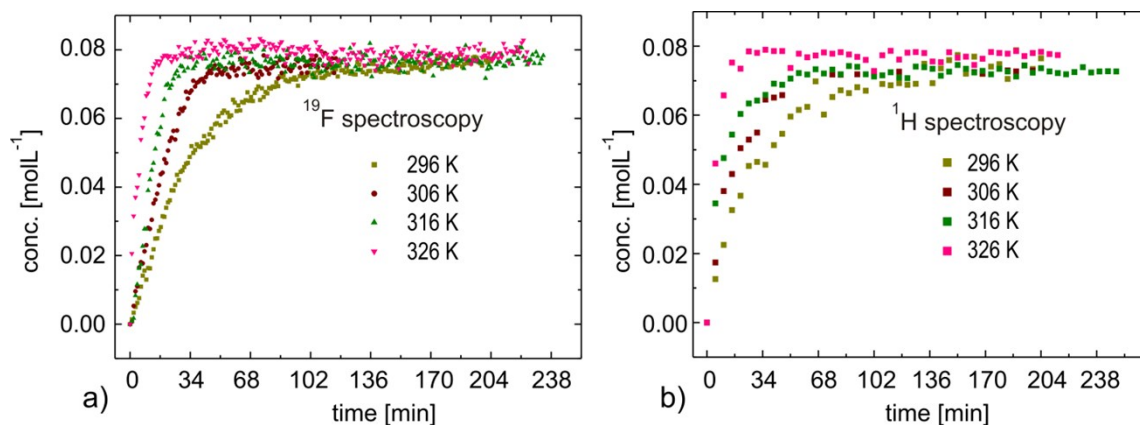
Figure S10: Hydrolysis of ethyl trifluoroacetate for temperatures ranging from 296 K to 326 K at 200 rpm agitation speed. a) Evolution of the concentration of trifluoromethyl group of the trifluoroacetic acid product followed with ^{19}F NMR spectroscopy. b) Evolution of the oxymethylene protons of the ethanol product followed with ^{1}H NMR spectroscopy.

11 Kinetic model for hydrolysis of ethyl trifluoroacetate obtained using 1D ^{1}H
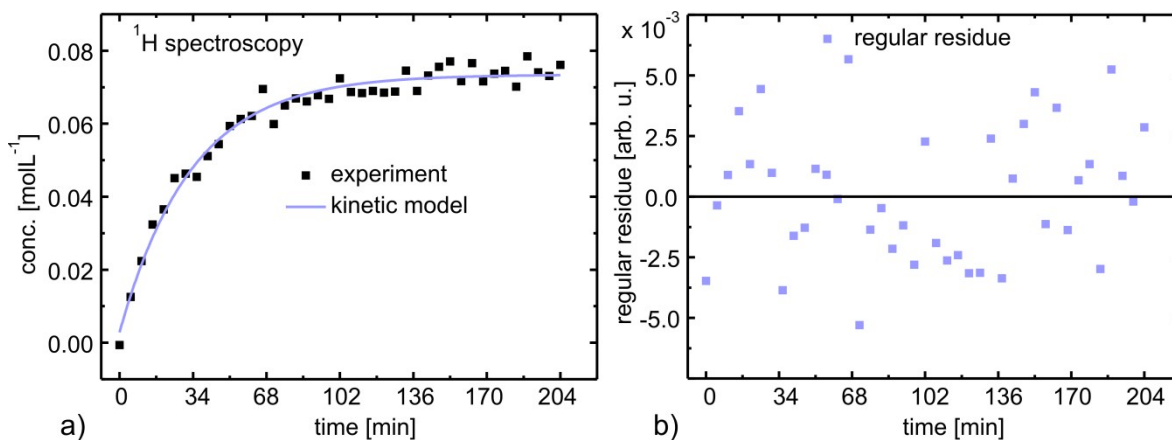
Figure S11: a) Kinetic model fitted with the experimental results obtained for the concentration of the oxomethylene (-OCH$_2$) group of ethanol (product). b) Residual regression obtained from fitting the kinetic model.

NMR spectroscopy

12   Proton inventory studies for hydrolysis of ethyltrifluoroacetate
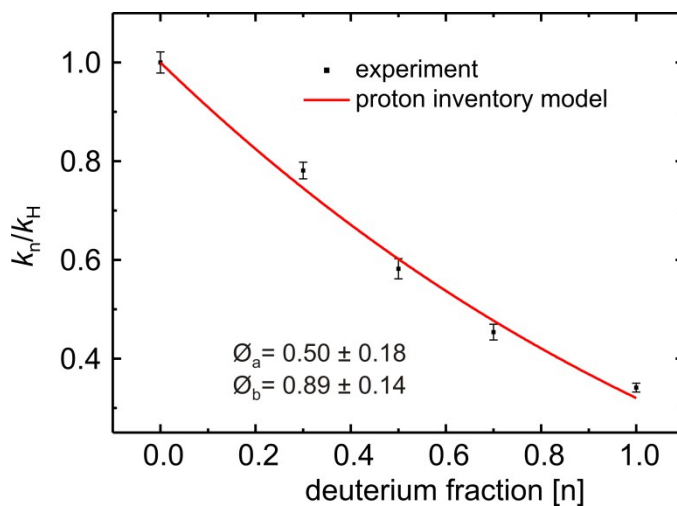
Figure S12: Proton inventory curve according to the Gross-Butler equation (8) for different atomic fractions of deuterium for hydrolysis of ethyltrifluoroacetate.

13   Repeatability measurements for the hydrolysis of acetic anhydride at 294 K

Table S1: Repeatability measurements for the hydrolysis of acetic anhydride at 294K

S. No.	$k \times 10^3$ [s^{-1}]
1	2.39 ± 0.0130
2	2.48 ± 0.0166
3	2.46 ± 0.0161
4	2.48 ± 0.0213
5	2.41 ± 0.0122
6	2.47 ± 0.0199

14 Activation enthalpies and entropies for the hydrolysis of acetic anhydride

Table S2: Activation enthalpies and entropies for the hydrolysis of acetic anhydride in H_2O and D_2O in the temperature range from 294 to 317 K.

Solvent	ΔH [kJ/mol]	$\Delta S^{\ddagger}$ [J/(K mol)]
H_2O	39 ± 2	-164 ± 7
D_2O	45 ± 2	-152 ± 6

15 Isotopic fractionation factors obtained for hydrolysis of acetic anhydride

Table S3: Isotopic fractionation factors obtained from fitting the Gross-Butler equation (9) to rate constants data obtained from different atomic fraction of deuterium.

			R^2
1.4	0.5 ± 0.52	0.70 ± 0.35	0.918
1.35	0.5 ± 0.41	0.73 ± 0.27	0.953
1.3	0.5 ± 0.29	0.75 ± 0.19	0.978
1.1	0.5 ± 0.08	0.76 ± 0.06	0.998
1	0.5 ± 0.17	0.78 ± 0.12	0.991
0.98	0.5 ± 0.15	0.80 ± 0.06	0.997
0.8	0.5 ± 0.04	0.87 ± 0.03	0.999
0.7	0.49 ± 0.03	0.94 ± 0.03	0.999
0.67	0.49 ± 0.03	0.95 ± 0.03	0.998

16 Activation energies for the hydrolysis of ethyltrifluoroacetate with 1D ^{1}H and ^{19}F NMR

Table S4: Activation energies (kJ/mol) for the reaction of ethyl trifluoroacetate with H_2O and D_2O obtained with ^{1}H and ^{19}F spectroscopy.

Solvent	^{19}F Spectroscopy	R^2	^{1}H Spectroscopy	R^2
H_2O	46.7 ± 1	0.998	48 ± 3	0.996
D_2O	54.9 ± 1	0.998	55.8 ± 1	0.998

17 Activation enthalpies and entropies for the hydrolysis of ethyltrifluoroacetate

Table S5: Thermodynamic parameters and for the hydrolysis of ethyl trifluoroacetate in H_2O and D_2O in the temperature range from 296 to 326 K derived from ^{19}F and ^{1}H NMR data.

Solvent	^{19}F spectroscopy		^{1}H spectroscopy	
	$\Delta H^{\ddagger}$ [kJ/mol]	$\Delta S^{\ddagger}$ [J/(K mol)]	$\Delta H^{\ddagger}$ [kJ/mol]	$\Delta S^{\ddagger}$ [J/(K mol)]
H_2O	45 ± 3	-155 ± 8	45 ± 3	-156 ± 8
D_2O	53 ± 1	-137 ± 4	53 ±1	-136 ± 3

18 Rate constants for the hydrolysis of ethyltrifluoroacetate at different atomic fractions of deuterium at 294 K

Table S6: Rate constants for the hydrolysis of ethyltrifluoroacetate at different atomic fractions of deuterium at 294 K.

S. No.	$[D_2O]$	$[H_2O]$	$k \times 10^4$ [s^{-1}]
1	0	100	5.16 ± 0.05
2	30	70	4.03 ± 0.05
3	50	50	3.00 ± 0.07
4	70	30	2.34 ± 0.06
5	100	0	1.76 ± 0.03

19 Isotopic fractionation factors obtained for hydrolysis of acetic anhydride

Table S7: Isotopic fractionation factors obtained from fitting the Gross-Butler equation (9) to rate constants data obtained from different atomic fraction of deuterium.

Φ^n	$\emptyset_a^*$	$\emptyset_b^*$	R^2
1.4	0.5 ± 0.38	0.70 ± 0.25	0.974
1.3	0.5 ± 0.31	0.71 ± 0.21	0.983
1.2	0.5 ± 0.32	0.72 ± 0.22	0.981
1.05	0.5 ± 0.92	0.70 ± 0.61	0.916
1.1	0.5 ± 0.27	0.76 ± 0.19	0.982
1	0.5 ± 0.76	0.73 ± 0.52	0.927
0.95	0.5 ± 0.64	0.76 ± 0.45	0.917
0.9	0.5 ± 0.54	0.79 ± 0.38	0.930
0.85	0.5 ± 0.45	0.82 ± 0.34	0.940
0.8	0.5 ± 0.18	0.89 ± 0.14	0.985

20 Temperature dependence of the kinetic isotope effect for hydrolysis of acetic anhydride

Table S8: Temperature dependence of the kinetic isotope effect for the reaction of acetic anhydride in H_2O and D_2O in the temperature range from 294 K to 317 K via ^{1}H NMR spectroscopy.

T [K]	k_{H_2O}/k_{D_2O}	uncertainty	k_{H_2O}/k_{HDO}	uncertainty
294	3.33	0.03	1.98	0.05
300	3.10	0.03	1.75	0.06
306	2.97	0.05	1.65	0.07
311	2.84	0.08	1.52	0.07
317	2.76	0.07	1.42	0.09

21 Temperature dependence of the kinetic isotope effect for hydrolysis of ethyltrifluoroacetate

Table S9: Temperature dependence of kinetic isotope effect for the reaction of ethyltrifluoroacetate with H_2O and D_2O at the temperature range of 296 K to 326 K obtained by using consecutive ^{1}H -^{19}F NMR spectroscopy.

T [K]	[19]F spectroscopy		[1]H spectroscopy	
	k_{H_2O}/k_{D_2O}	k_{H_2O}/k_{HDO}	k_{H_2O}/k_{D_2O}	k_{H_2O}/k_{HDO}
296	2.93 ± 0.08	2.02 ± 0.15	2.95 ± 0.20	1.97 ± 0.43
306	2.74 ± 0.13	1.78 ± 0.20	2.75 ± 0.17	1.77 ± 0.31
316	2.26 ± 0.09	1.44 ± 0.13	2.20 ± 0.14	1.62 ± 0.26
326	2.24 ± 0.13	1.39 ± 0.16	2.25 ± 0.14	1.60 ± 0.28